Math. Program., Ser. B (2015) 151:347–373
DOI 10.1007/s10107-015-0887-0

FULL LENGTH PAPER

Transmission system repair and restoration

P. Van Hentenryck[1] · **C. Coffrin**[1]

Received: 15 October 2014 / Accepted: 17 February 2015 / Published online: 18 March 2015

Abstract This paper studies the use of mathematical programming for the repair and restoration of a transmission system after a significant disruption (e.g., a natural disaster). Such blackouts may last several days and have significant impact on human and economic welfare. The transmission system repair and restoration problem (TSRRP) consists in dispatching crews to repair damaged electrical components in order to minimize the size of the blackout. The TSRRP can be modeled as a large-scale mixed nonlinear, nonconvex program, including both routing components and the nonlinear steady-state power flow equations. To tackle its daunting computational complexity, this paper proposes a 2-stage approach, decoupling the restoration and repair aspects. The first step is a restoration ordering problem, a mixed nonlinear, nonconvex program which is approximated by a mixed integer program. The approximation does not use the traditional DC power flow approximation which is plagued by convergence issues and inoperable dispatches; rather, it uses the recent LPAC approximation that captures reactive power and voltage magnitudes. The second stage is a pickup and repair routing problem which is solved using a constraint-programming model, large neighborhood search, and a randomized adaptive decomposition. Experimental results on benchmarks based on the US electrical infrastructures and state-of-the-art damage scenarios indicate that the 2-stage approach provides significant improvements over the "best practice" in the field.

Mathematics Subject Classification 90-08 · 90C11 · 90C59 · 90C90 · 68T20

✉ P. Van Hentenryck
pascal.vanhentenryck@nicta.com.au; pvh@nicta.com.au

C. Coffrin
Carleton.Coffrin@nicta.com.au

[1] National ICT Australia (NICTA), Australian National University, Canberra, Australia

1 Introduction

Restoring a power system after a significant disruption (e.g., a natural disaster) is an important task with potentially significant consequences on both human and economic welfare. On the economic side, for instance, the losses from the San Diego 24-h blackout in 2011 were estimated to be around 100 million dollars. Major hurricanes such as Irene and Sandy frequently cause blackouts lasting close to or over a week and leaving major sections of the population without air-conditioning, heating, refrigeration, lighting, and telecommunication devices. It is thus not surprising that power restoration is a major part of disaster recovery. The "best practice" in the field for power restoration uses relatively simple optimization technique: It implements a restoration order dictated by the US government and based on network utilization heuristics and then uses an agent-based greedy routing algorithm that satisfies the restoration order.

This paper studies the potential benefits of mathematical programming for the repair and restoration of the transmission system after such a major disruption. The objective is to dispatch crews to repair grid components as quickly as possible in order to minimize the size of the blackout over time. Observe that major blackouts typically span multiple days, as was the case for Hurricane Irene in 2011 for instance. The transmission system repair and restoration problem (TSRRP) is a daunting problem, even when ignoring transient effects and focusing on the steady-state behavior of the power grid. When modeled globally, it is a large-scale mixed nonlinear, nonconvex optimization problem. Moreover, the two subproblems of the TSRRP, the scheduling of the repair and the sequencing of the restoration, are computationally challenging in their own right. The repair scheduling is equivalent to a pickup and delivery vehicle routing minimizing the sum of the delivery completion dates.

This paper shows how to use mathematical programming to improve the "best practices" in the field. It proposes a scalable algorithm to the TSRRP based on a 2-stage approach decoupling the power restoration and the routing aspects. The first stage is a restoration ordering problem that finds the restoration sequence that minimizes the blackout size, ignoring the logistics of scheduling the repairs. The second stage is a large-scale pickup and repair routing problem enforcing the restoration prioritizations computed in the first stage. Both stages are computationally challenging in their own right.

The restoration problem is a mixed nonlinear nonconvex optimization problems since it captures the power flow equations for active and reactive power. In addition, contrary to traditional optimal power flow problems, during which the grid operates in normal conditions, power restoration takes place when the grid is damaged and when the objective is to serve as much load as possible. Finding solutions to the power flow equations in such a context raises significant challenges [25]. A key contribution of this paper is to show that the restoration problem can be approximated by a Mixed-Integer Program (MIP) that linearizes the power flow equations. The linearization is non-standard however: Indeed, the paper shows that the traditional DC power flow approximation (e.g., [8,10,25,29]) is plagued by convergence issues or generates inoperable generator dispatches. The convergence issues arise when a

Table 1 Gloassary for the main problems and models

Abbreviation	Meaning	Text reference
AC-LPP	AC load pickup problem	Model 1
DC	DC approximation	Section 5.1
LPAC	LPAC approximation	Section 5.2
DC-LPP	DC load pickup problem	Section 5.3
LPAC-LPP	LPAC load pickup problem	Section 5.3
TSRRP	Transmission system repair and restoration problem	Section 2.3
ROP	Restoration ordering problem	Section 4
AC-ROP	Restoration ordering problem: AC model	Model 2
DC-ROP	Restoration ordering problem: DC model	Section 5.3
LPAC-ROP	Restoration ordering problem: LPAC model	Section 5.3
PRRP	Pickup and repair routing problem	Model 3

nonlinear solver (e.g., a Newton–Raphson algorithms) is seeded with the results of the DC Model (e.g., the computed real power at the buses) and failed to converge when computing the remaining variables (e.g., the bus phase angles). To remedy this limitation, the paper uses the LPAC model, a linear-programming approximation to the power flow equations that captures both reactive power and voltage magnitudes.

The second-stage is a large-scale routing problem which is modeled as a constraint program. The paper shows that this constraint program, together with a large-neighborhood search and a randomized adaptive decomposition, provides a scalable approach to scheduling the repairs.

The approach was validated on benchmarks using the United States electricity infrastructures and disaster scenarios based on state-of-the-art simulation tools for damage generation [13]. The experimental results demonstrate that the mathematical-programming approach brings substantial improvements over the "best practices" in the field, often reducing the size of the blackout by 30–40 %.[1] Equally importantly, the paper sheds new light on how to approximate the power flow equations, providing a cautionary tale on the use of the DC power flow model in contexts where the network is stressed.

The rest of the paper is organized as follows. Section 2 specifies the TSRRP and reviews prior art in transmission system restoration. Section 3 gives an overview of the 2-stage decomposition. Section 4 presents the restoration ordering problem and Sect. 5 studies its key building block, the load pickup problem (LPP). Section 6 gives an overview of the pickup and repair routing problem. Section 7 concludes the paper. Table 1 provides a glossary of the optimization problems and models presented in the paper.

[1] The algorithms presented in this paper were deployed through our collaboration with the Los Alamos National Laboratory and activated during hurricanes Irene and Sandy to help federal agencies in the United States.

Model 1 The AC load pickup problem (AC-LPP).

Inputs:

$\mathcal{P} = \langle N, L \rangle$	- the power network
g_{nm}, b_{nm}	- admittance between bus n and bus m
p_n^l, q_n^l	- desired active and reactive loads at bus n
S_{nm}	- line loading limit on line (n, m)

Variables:

$\theta_n \in (-\infty, \infty)$	- phase angle of bus n (radians)
$v_n \in [\underline{v_n}, \overline{v_n}]$	- voltage magnitude of bus n
$p_n^g \in [\underline{p_n^g}, \overline{p}_n^g]$	- active generation at bus n
$q_n^g \in [\underline{q_n^g}, \overline{q}_n^g]$	- reactive generation at bus n
$l_n \in [0, 1]$	- percentage load served at bus n
$p_{nm} \in [-S_{nm}, S_{nm}]$	- active power on line (n, m)
$q_{nm} \in [-S_{nm}, S_{nm}]$	- reactive power on line (n, m)

Maximize:

$$\sum_{n \in N} p_n^l l_n \tag{M1.1}$$

Subject to:

$$p_n^g - p_n^l l_n = \sum_{(n,m) \in L} p_{nm} \qquad (n \in N) \tag{M1.2}$$

$$q_n^g - q_n^l l_n = \sum_{(n,m) \in L} q_{nm} \qquad (n \in N) \tag{M1.3}$$

$$p_{nm} = v_n^2 g_{nm} - v_n v_m g_{nm} \cos(\theta_n - \theta_m) - v_n v_m b_{nm} \sin(\theta_n - \theta_m) \qquad ((n, m) \in L) \tag{M1.4}$$

$$q_{nm} = -v_n^2 b_{nm} + v_n v_m b_{nm} \cos(\theta_n - \theta_m) - v_n v_m g_{nm} \sin(\theta_n - \theta_m) \qquad ((n, m) \in L) \tag{M1.5}$$

$$p_{nm}^2 + q_{nm}^2 \leq S_{nm}^2 \quad ((n, m) \in L) \tag{M1.6}$$

2 Problem specification

2.1 The power network

The power network $\mathcal{P} = \langle N, L \rangle$ is defined in terms of a set N of buses and a set L of lines. A bus n is characterized by its desired active and reactive loads denoted by p_n^l and q_n^l, its limits on active and reactive generation which must be in the intervals $[\underline{p_n^g}, \overline{p}_n^g]$ and $[\underline{q_n^g}, \overline{q}_n^g]$ respectively, and its limits on voltage magnitudes which must be within $[\underline{v_n}, \overline{v_n}]$. Each line (n, m) between buses n and m is characterized by its admittance $g_{nm} + i b_{nm}$ and its capacity S_{nm}. The admittance of a line (n, m) is a complex number composed of the conductance g_{nm} and the susceptance b_{nm}. In power restoration, a subset of network components have been damaged and must be repaired and re-activated. For simplicity, we restrict attention to a set R of damaged lines in this paper, but the models generalize naturally to other components [36].

2.2 Optimization of load pickups

The LPP is the core sub-problem of transmission system restoration. Its goal is to supply as much active power as possible to the load points of a power network. The LPP is used to specify the objective function in transmission system repair and restoration; it is also a key component of our solution method.

An LPP formulation using the steady-state AC power flow equations is presented in Model 1. The AC-LPP departs from optimal power flow problems in that the loads are decision variables: The goal of the model is to determine how much load is served and how. The main decision variables are

- variable l_n which denotes the percentage of the active and reactive loads served at bus n;
- variables p_n^g and q_n^g which denote the active and reactive power injections at bus n;
- variables v_n and θ_n which represent the voltage magnitude and phase angle at bus n.

The objective (M1.1) maximizes the active load. Constraints (M1.2–M1.3) capture flow conservation (i.e., Kirchhoff's Current Law). Constraints (M1.4–M1.5) define the real and reactive power flows on lines and constraints (M1.6) enforce the thermal limits for lines.

Model 1 assumes that the loads are continuous quantities and that their power factor is maintained during restoration. The power factor is the ratio between the active power and apparent power and is maintained in the model by scaling active and reactive power injections by the same percentage (variable l_n for bus n). This AC-LPP formulation can be generalized to include discrete loads or prioritized power demands: It suffices to discretize the l_n variables and/or to weight the objective function appropriately.

2.3 Transmission system repair and restoration

TSRRP is defined in terms of a power network $\mathcal{P}$ with a set R of damaged components and a graph $G = \langle S, E \rangle$ where S represents sites of interest for the restoration and E are the arcs between sites. The sites are of four types: (1) the depots H^+ at which repair vehicles depart; (2) the depots H^- at which repair vehicles must return; (3) the depots W^+ where stockpiled resources are located; and (4) the locations W^- of the lines in R. Due to infrastructure damages, the travel times on the edges are typically not Euclidean, but form a metric space. For simplicity, this paper assumes that the graph is complete and $t_{i,j}$ denotes the distance between sites i and j.

The routing component The repair process has at its disposal a set V of vehicles. Each vehicle $v \in V$ is characterized by its departure depot h_v^+, its returning depot h_v^-, and its capacity c_v. Vehicle v starts from h_v^+, performs a number of repairs, and returns to h_v^-. A vehicle cannot carry more resources than its capacity.

The repair process must complete a set J of restoration jobs. Each job j is characterized by a pickup location $p_j^+ \in W^+$, a repair location $p_j^- \in W^-$, a weight d_j, a service time s_j, and a line $n_j \in R$. Performing a job consists of picking up repair supplies at p_j^+ which uses d_j units of the vehicle capacity, traveling to site p_j^-, and repairing line n_j for a duration s_j. After completion of job j, network item n_j is operational and can be activated.

A solution to the TSRRP associates a route with each vehicle such that all locations are visited exactly once. A solution can then be viewed as assigning to each site $i \in H^+ \cup W^+ \cup W^-$, a vehicle $vehicle_i$ visiting i, the weight $weight_i$ of the vehicle

when visiting i, the next destination of the vehicle (i.e., the successor σ_i of i in the route of $vehicle_i$), and the earliest departure time edt_i of the vehicle at location i. The weights at the sites can be defined recursively as follows:

$$\begin{array}{ll} weight_i & = 0 \quad \text{if } i \in H^+ \\ weight_{\sigma_i} & = weight_i + d_i \quad \text{if } i \in W^+ \\ weight_{\sigma_i} & = weight_i - d_i \quad \text{if } i \in W^-. \end{array}$$

Pickup sites increase the weight, while repair sites decrease it. The earliest arrival time at a site i can be defined recursively as

$$\begin{array}{ll} eat_i & = 0 \quad \text{if } i \in H^+ \\ eat_{\sigma_i} & = eat_i + t_{i,\sigma_i} \quad \text{if } i \in W^+ \\ eat_{\sigma_i} & = eat_i + t_{i,\sigma_i} + s_i \quad \text{if } i \in W^-. \end{array}$$

The earliest arrival time of a location is the earliest arrival time of its predecessor plus the travel time and the service time for repair locations. The earliest departure time edt_i from a site i is simply the earliest arrival time to which the service time is added for repair locations. A solution must satisfy the following constraints:

$$\begin{array}{lll} vehicle_{p_j^+} & = vehicle_{p_j^-} & \forall j \in J \\ eat_{p_j^+} & < eat_{p_j^-} & \forall j \in J \\ weight_i & \leq c_{vehicle_i} & \forall i \in W^+ \cup W^-. \end{array}$$

The first constraint specifies that the same vehicle performs the pickup and repair visits of a given job, the second constraint ensures that a repair takes place after its pickup, while the third constraint makes sure that the vehicle capacities are never exceeded. Note that the service and travel times play a significant role in the objective function.

The TSRRP objective minimizes the size of the blackout in watts/hours or, equivalently, maximizes the load served over time. Since the repair actions occur at discrete times, the objective can be written as

$$\sum_{i=2}^{|R|} L_{i-1} \ (edt_{r_i} - edt_{r_{i-1}})$$

where r_i is the site of the ith repaired line and L_i is the load after the ith line has been repaired. This load can be computed in terms of the LPP. Let $\mathcal{P} = \langle N, L \rangle$ be the power system, R be the set of damaged lines, and $L^o = L \backslash R$. The load at step i can be defined as

$$L_i = LPP(\langle N, L^o \cup R_i \rangle)$$

where R_i are all the lines repaired at step i. In fact, since power systems exhibit Braess paradox (e.g., adding a line may decrease the served load), the above expression should be replaced by

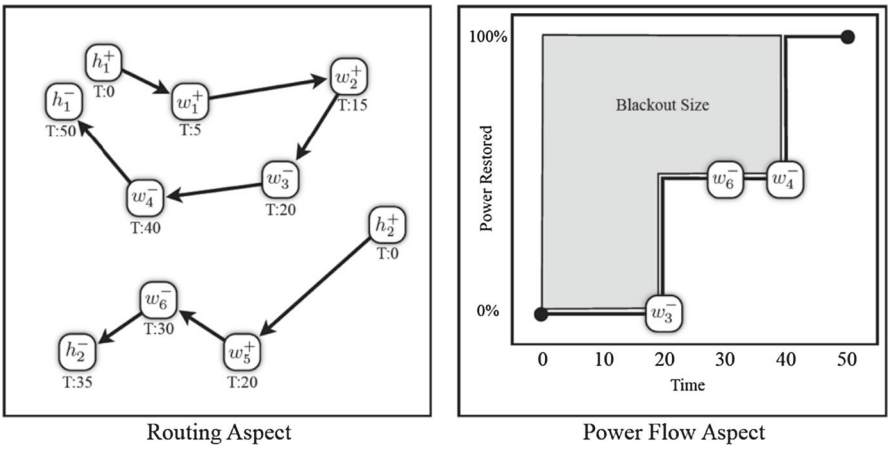

Fig. 1 Illustrating transmission system restoration

$$L_i = \max_{S \subseteq R_i} LPP(\langle N, L^o \cup S \rangle). \tag{1}$$

Illustration Figure 1 illustrates the TSRRP, highlighting the joint routing and power system aspects. The left part of the figure depicts the routing which consists of two repair crews (vehicles). The right part of the figure depicts the blackout and served load (y-axis) over time (x-axis). The first vehicle starts from its depot, picks up parts at sites w_1^+ and w_2^+ at times 5 and 15, and repairs the line at site w_3^- at time 20. Observe that, in the right figure, the served load increases after the w_3^- visit. The second crew repairs the line in site w_6^- at time 30 but this repair alone does not increase the served load. It is only when the first crew repairs the line at site w_4^- at time 40 that the full load is served.

Computational considerations The TSRRP is extremely challenging from a computational standpoint, since it is composed of two subproblems which are challenging in their own right. On the one hand, pickup and delivery vehicle-routing problems have been studied for a long time in operations research. For reasonable sizes, they are rarely solved to optimality. In particular, when the objective is to minimize the average delivery time (which is related to the TSRRP objective), Campbell et al. [9] have shown that MIP approaches have serious scalability issues. On the other hand, maximizing the served load in Eq. (1) generalizes optimal transmission switching which has been shown to be challenging for MIP solvers [14], even when using linear approximations of the power flow equations. Therefore, it is highly unlikely that a direct approach, combining MIP models for both the routing and power flow subproblems, would scale to the size of even small restorations. Our experimental results with such an approach were in fact very discouraging, which is not surprising given the above considerations.

2.4 Prior art

Power system restoration (PSR) has been an area of active research for at least 30 years (see [1] for a comprehensive collection of work). Its goal is to find fast and reliable

ways of restoring a power system to its normal operational state after many components have been damaged or disconnected (e.g., after a cascading blackout). Due to the complex nature of power systems, PSR remains challenging. Practitioners must delicately manipulate many aspects of the network, including power balance, line thermal limits, power quality, generator ramp rates, and transient effects. In general, these challenges form a loose priority list: Power balance must be ensured first before considering line thermal limits and so on. This paper focuses on power balance, line limits, and power quality, leaving additional aspects for future consideration. Extensions of this work to capture aspects of transient stability are proposed in [16,21].

Even when ignoring transient stability, the PSR research community has recognized that global optimization is often impractical for such complex non-linear systems and adopted two main solutions strategies. The first strategy is to use domain-expert knowledge (i.e., power engineer intuition) to guide an incomplete search of the solution space. These incomplete search methods include *knowledge-based and expert systems* [3,4,17,28] and *local search* [22,23]. The second strategy is to approximate the power system with a linear model and to try solving the approximate problem optimally [12,14,38]. Some work hybridized both strategies by designing expert systems that solves a series of approximate problems optimally [18,24]. Observe however that most PSR work assumes that all network components are operational and "only" need to be reactivated (e.g., [2,3]).

3 The decomposition approach

To address the computational difficulties of the TSRRP, this paper explores a decomposition approach that decouples the repair and restoration aspects of the TSRRP. The decomposition is based on the insight that a repair schedule with a small blackout size is characterized by an underlying high-quality restoration order.

More precisely, the first step of the decomposition consists in solving a restoring ordering problem (ROP) which abstracts away all routing components. The ROP considers a time horizon $1..|R|$ and assumes that only one component $r \in R$ can be repaired at each time step. It determines a restoration order $\langle r_1, \ldots, r_{|R|} \rangle$ for all the damaged components in R that minimizes the size of the blackout. The second step of the decomposition is a Pickup and Repair Routing Problem (PRRP) that receives, as input, a set of precedence constraints that capture a partial order on the repairs derived from the ROP solution. The PRRP minimizes the sum of the the completion times of the repair visits, which is a good proxy for the blackout size given that the precedence constraints enforce an optimal restoration schedule.

The decomposition is specified in Fig. 2. The ROP and the PRRP are described in full detail in subsequent sections, since they constitute the core of the approach. Before specifying how the precedence constraints are generated from the ROP solution (Step

Fig. 2 The decomposition algorithm for the TSRRP

TSRRP(*Network* $\mathcal{P}$, *Graph* G)
1 $\mathcal{O} \leftarrow ROP(\mathcal{P}, R)$;
2 $\mathcal{C} \leftarrow ComputePrecedences(\mathcal{O})$;
3 **return** $PRRP(G, \mathcal{C})$.

2 in in Fig. 2), recall that several repairs may be necessary before more load can be served, as is illustrated in Fig. 1. As a result, the ROP solution $\langle r_1, \ldots, r_{|R|} \rangle$ is best viewed as a partition of R into m sets $R_1, \ldots, R_m$, where $R_i = \{r_{s_i}, \ldots, r_{e_i}\}$ and

$$\langle r_1, \ldots, r_{|R|} \rangle = \langle r_{s_1}, \ldots, r_{e_1}, \ldots, r_{s_m}, \ldots, r_{e_m} \rangle.$$

The partition ensures that the served load increases after each repair in a set R_i has been completed. As a result, it is only necessary to impose precedences between jobs whose repairs appear in two consecutive sets, i.e.,

$$\mathcal{C} = \{i \rightarrow j \mid p_i^- \in R_i \ \& \ p_j^- \in R_{i+1}\}.$$

The routing satisfies a precedence constraint $i \rightarrow j$ between jobs i and j if $eat_{p_i^-} \leq eat_{p_j^-}$. It is important to note that the ordering of a set is not important from a restoration standpoint: All the components must be restored to serve more load. However, the ordering of the set may be significant for the routing problem and hence the resulting flexibility improves the overall restoration.

4 The restoration ordering problem

The intuition underlying the ROP is depicted visually in Fig. 3. The ROP receives as input the power network $\mathcal{P}$ and the set R of components to repair. It considers $|R|$ restoration steps and selects a component $n \in R$ for each restoration step. After each step k, the ROP computes the steady state of the power network $\mathcal{P}$ maximizing the served load. In other words, the ROP can be viewed as searching for a sequence

$$r_1 \rightarrow r_2 \rightarrow \cdots \rightarrow r_{|R|}$$

of the damaged components in R. The sequence of restoration steps is associated with a sequence of steady states for the power system

$$S_1 \rightarrow S_2 \rightarrow \cdots \rightarrow S_{|R|}$$

where steady state S_i corresponds to the damaged network where the components $\{r_1, \ldots, r_i\}$ have been repaired. The goal of the ROP is to minimize the blackout size

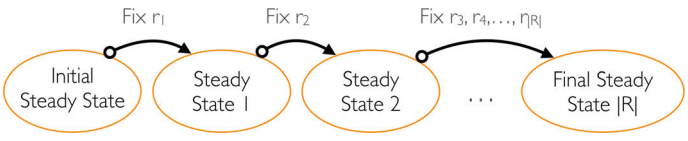

Fig. 3 The intuition underlying the restoration ordering problem

Model 2 The AC restoration ordering problem (AC-ROP).

Inputs:

$\mathcal{P} = \langle N, L \rangle$	- the power network
g_{nm}, b_{nm}	- admittance between bus n and bus m
p_n^l, q_n^l	- desired active and reactive load at bus n
S_{nm}	- line loading limit on line (n, m)
R	- the set of lines to repair

Variables:

$o_{nmk} \in \{0, 1\}$	- line (n, m) is repaired at step k
$z_{nmk} \in \{0, 1\}$	- line (n, m) is activated at step k
$\theta_{nk} \in (-\infty, \infty)$	- phase angle of bus n (radians) at step k
$v_{nk} \in [\underline{v_n}, \overline{v_n}]$	- voltage magnitude of bus n at step k
$p_{nk}^g \in [\underline{p_n^g}, \overline{p_n^g}]$	- active generation at bus n at step k
$q_{nk}^g \in [\underline{q_n^g}, \overline{q_n^g}]$	- reactive generation at bus n at step k
$l_{nk} \in [0, 1]$	- percentage load served at bus n at step k
$p_{nmk} \in [-S_{nm}, S_{nm}]$	- active power on line (n, m) at step k
$q_{nmk} \in [-S_{nm}, S_{nm}]$	- reactive power on line (n, m) at step k

Maximize:

$$\sum_{k=1}^{|R|} \sum_{n \in N} p_n^l l_{nk} \tag{M2.1}$$

Subject to: $(1 \leq k \leq |R|)$

$$\sum_{(n,m) \in R} o_{nmk} = k \tag{M2.2}$$

$$o_{nmk-1} \leq o_{nmk} \qquad ((n, m) \in R) \tag{M2.3}$$

$$z_{nmk} \leq o_{nmk} \qquad ((n, m) \in R) \tag{M2.4}$$

$$z_{nmk} = 1 \qquad ((n, m) \in L \backslash R) \tag{M2.5}$$

$$p_{nk}^g - p_n^l l_{nk} = \sum_{(n,m) \in L} p_{nmk} \qquad (n \in N) \tag{M2.6}$$

$$q_{nk}^g - q_n^l l_{nk} = \sum_{(n,m) \in L} q_{nmk} \qquad (n \in N) \tag{M2.7}$$

$$\begin{aligned} z_{nmk} \rightarrow p_{nmk} = v_{nk}^2 g_{nm} &- v_{nk}\, v_{mk}\, g_{nm}\, \cos(\theta_{nk} - \theta_{mk}) \\ &- v_{nk}\, v_{mk}\, b_{nm}\, \sin(\theta_{nk} - \theta_{mk}) \qquad ((n, m) \in L) \end{aligned} \tag{M2.8}$$

$$\begin{aligned} z_{nmk} \rightarrow q_{nmk} = -v_{nk}^2 b_{nm} &+ v_{nk}\, v_{mk}\, b_{nm}\, \cos(\theta_{nk} - \theta_{mk}) \\ &- v_{nk}\, v_{mk}\, g_{nm}\, \sin(\theta_{nk} - \theta_{mk}) \qquad ((n, m) \in L) \end{aligned} \tag{M2.9}$$

$$\neg z_{nmk} \rightarrow p_{nmk} = 0, q_{nmk} = 0 \qquad ((n, m) \in L) \tag{M2.10}$$

$$p_{nmk}^2 + q_{nmk}^2 \leq S_{nm}^2 \qquad ((n, m) \in L) \tag{M2.11}$$

over time, which is equivalent to maximizing

$$\sum_{k=1}^{|R|} \sum_{n \in N} p_n^l l_{nk}$$

where l_{nk} is the portion of the load at the bus n served in the state steady state S_k following restoration step k.

Figure 2 depicts a mixed nonlinear model for the ROP. Intuitively, the ROP model consists of $|R|$ replications of the LPP model linked together by constraints ensuring that each step restores a single damaged line. Each step $k \in 1 \ldots |R|$ features the same decision variables as the LPP: For instance, variable l_{nk} denotes the percentage of the load served at bus n at step k, while variables p_{nmk} denotes the active power on

line (n, m) at step k. In addition, the ROP includes some new variables: o_{nmk} denotes whether line (n, m) is repaired at step k and variable z_{nmk} represents whether the line is activated at step k. This allows the algorithm to deal with Braess paradox by delaying the activation of line (n, m) even if it is repaired.[2] The power flow constraints for a line (n, m) are now only imposed at step k if the line is activated, i.e., if $z_{nmk} = 1$. This is captured by constraints (M2.8–M2.10). In addition, constraints (M2.2–M2.3) ensure that exactly one line is repaired at each step k, constraints (M2.4) make sure that damaged lines are activated only if they are repaired, while constraints (M2.5) specify that all lines that are not damaged are activated.

Although it abstracts away the repair aspects, the ROP is still challenging computationally for two main reasons. On the one hand, it is highly combinatorial as it aims at finding a sequence of steady states minimizing the blackout size over time. On the other hand, finding the steady states themselves is not a easy task: Each steady state is in fact specified by an LPP which is a nonlinear program. We now study how to address the second difficulty.

5 Approximating the load pickup problem

The AC-LPP model (see Fig. 1) is the core subproblem of the ROP and is a nonlinear non-convex program which could be submitted to nonlinear solvers such as IPOPT [37]. However, such an approach raises two fundamental difficulties:

1. Such (local) nonlinear solvers are not guaranteed to converge to a feasible solution, especially in the context of the LPP which is pushing the system to accommodate as much load as possible. Indeed, under stress, the solution space is riddled with infeasible low-voltage solutions which are not usable in practice [34]. Moreover, finding a solution to the AC power flow equations in cold-start contexts [32] is known to be "maddeningly difficult" [25].
2. The LPP is a building block of the ROP, which contains both continuous and discrete aspects.

To address these difficulties, this paper explores linearizations of the power flow equations (M1.4) and (M1.5), making it possible to use standard mixed-integer programming technology for the ROP.

5.1 The DC approximation

The DC model [20] is the most common linear approximation of the power flow equations and has been used in many power system applications (e.g., [8,10,25,29]). It consists in replacing constraints (M1.4–M1.5) by

$$p_{nm} = -b_{nm}(\theta_n - \theta_m).$$

[2] Note that the combination of delaying an activation and enforcing that a line remains activated provide a practical and acceptable way to address Braess paradox.

The DC model is derived through a number of simplifying assumptions. In particular, the derivation assumes that voltage magnitudes v_n and v_m are 1.0 in the per unit system, that reactive power is negligible compared to real power, and that the conductance g_{nm} is much smaller than the susceptance b_{nm}. In addition, the phase angle difference $\theta_n - \theta_m$ is assumed to be small, in which case $\sin(\theta_n - \theta_m) \approx \theta_n - \theta_m$. As a result, the DC model does not capture line losses, reactive power, and voltage magnitudes.

5.2 The LPAC approximation

In order to bridge the gap between the DC and AC power flow models, another linear-programming approximation of the AC power flow equations was proposed recently. The LPAC model [11] is derived from the AC power flow equations through both approximations and relaxation steps. It imposes that the phase angle differences satisfy $-\pi \leq \theta_n - \theta_m \leq \pi$, which is not restrictive in practice, and rewrites the voltage magnitude at each bus n as a deviation from a nominal operating voltage v^t, i.e., $v_n = v_n^t + \phi_n$. The relaxation step replaces the non-convex cosine function with a piecewise-linear relaxation denoted by $\widehat{\cos}$ and satisfying

$$\cos(\theta) \in \widehat{\cos}(\theta)$$

whenever $-\hat{\theta} \leq \theta \leq \hat{\theta}$ for $\hat{\theta} \in [0, \pi/2]$. The LPAC model also makes two approximations:

1. It replaces $\sin(\theta_n - \theta_m)$ by $\theta_n - \theta_m$ as in the DC model;
2. The remaining non-linear terms are then approximated with a first-order Taylor expansion.

As result, in the LPAC model, Equations (M1.10–M1.11) are replaced by

$$\begin{aligned} p_{nm} &= g_{nm} - g_{nm}\cos_{nm} - b_{nm}(\theta_n - \theta_m) \\ q_{nm} &= -b_{nm} + b_{nm}\cos_{nm} - g_{nm}(\theta_n - \theta_m) - b_{nm}(\phi_n - \phi_m). \end{aligned}$$

where $\cos_{nm} \in \widehat{\cos}(\theta_n - \theta_m)$. This last constraint is implemented by the set of constraints

$$\begin{aligned} &\cos_{nm} \geq \cos(\hat{\theta}) \\ &\cos_{nm} \leq -\sin(td - \hat{\theta})(\theta_n - \theta_m - td + \hat{\theta}) + \cos(td - \hat{\theta}) \qquad (t \in \{1..h\}) \end{aligned}$$

where h is the number of hyperplanes selected in the piecewise linear approaximation. The hyperplanes are evenly spaced in $[-\hat{\theta}, \hat{\theta}]$ with a distance $d = 2\hat{\theta}/(h+1)$.

The LPAC model is a linear program, yet it captures line losses, reactive power flows, and voltage magnitudes. These elements are important in power restoration as the computational results will demonstrate.

5.3 Computational results

This section studies the behavior of the LPP model when the power flow equations are approximated with the DC and LPAC models. In the following, we use AC-LPP, DC-LPP, and LPAC-LPP to denote the AC-LPP model and its two approximations. In both DC-LPP and LPAC-LPP, constraints (M1.6) are relaxed by taking a piecewise linear approximation of the quadratic terms.

Evaluating the quality of the approximations The DC-LPP and LPAC-LPP models are assessed experimentally using a two-stage evaluation algorithm:

1. Solve the approximate LPP model (DC-LPP or LPAC-LPP).
2. Construct an AC power flow problem with the generator dispatches and load pickups from Stage (1) and solve it with a nonlinear solver to obtain a solution to the AC power flow equations.

This evaluation algorithm applied to the DC-LPP and AC-LPP models is denoted by E-DC-LPP and E-LPAC-LPP respectively. The second step only considers the power flow equations and relaxes all other constraints, including the bounds on the decision variables. In other words, the optimization results of the first stage seeds a power flow study that is solved by a standard Newton–Raphson algorithm. The seeding uses different kinds of information depending on the bus types. For a P–Q bus, the real and reactive power injections are known and the complex voltage is a variable. For a P–V bus, the real power and the voltage magnitudes are known and the reactive power and the phase angles are variables. After solving the AC power flow, it is thus possible to measure these constraint violations and assess the quality of the respective approximations. Because the DC-LPP and LPAC-LPP models are linear, the first step of this approach is guaranteed to converge to a solution if one exists. The AC power flow problem in the second step is a system of nonconvex nonlinear equations and nonlinear methods such as Newton–Raphson are not guaranteed to converge to a feasible solution. The study of this convergence, or the absence thereof, is one of the key aspects of the experimental evaluation.

Reliability of the DC-LLP and AC-LLP We first evaluate the reliability of the DC-LPP and LPAC-LPP in isolation on the IEEE30 bus network. The evaluation considers 170,000 damage contingencies obtained by randomly selecting 10,000 damaged networks for each of the N-3, N-4, …, N-20 cases, where N–k denotes a network where k lines have been damaged. Table 2 reports how often DC-LLP and LPAC-LLP solutions converge to AC solutions. The second and the third columns show the number of solved models and the average active power dispatched, grouped by contingency size, for the DC-LPP model. The fourth and the fifth columns depict the same information for the LPAC-LPP model. For small contingencies (i.e., N-3 and N-4) where less than 10 % of the network is damaged, the E-DC-LPP algorithm almost always converges to an AC solution. However, for large contingencies (i.e., N-10 to N-14) where more than 25 % of the network is damaged, the DC-LPP solution only converts to an AC solution in about 78 % of the time. In contrast, the experimental results indicate that LPAC-LPP solutions convert to AC solutions in 99.5 % of the contingencies. Furthermore, this

Table 2 IEEE30 contingencies for the DC-LPP and LPAC-LPP models

Damage	E-DC-LPP		E-LPAC-LPP	
	Solved	μ (% delivered)	Solved	μ (% delivered)
N-3	9945	98.76	10,000	93.14
N-4	9846	97.48	9999	90.37
N-5	9652	95.96	9998	87.35
N-6	9401	93.79	9995	84.25
N-7	9048	91.02	9991	80.8
N-8	8720	87.2	9983	77.07
N-9	8291	83.4	9971	73.58
N-10	8022	78.67	9971	69.88
N-11	7801	73.56	9956	65.87
N-12	7683	68.82	9951	62.44
N-13	7832	63.06	9965	57.94
N-14	7920	58.06	9946	53.95
N-15	8154	52.19	9955	49.22
N-16	8472	48.23	9962	45.83
N-17	8724	44.18	9962	42.21
N-18	8973	40.84	9974	39.06
N-19	9197	36.58	9989	35.17
N-20	9463	33.65	9988	32.26

The table indicates the number of contingencies solved by the DC-LPP and LPAC-LPP models, both in absolute and relative terms

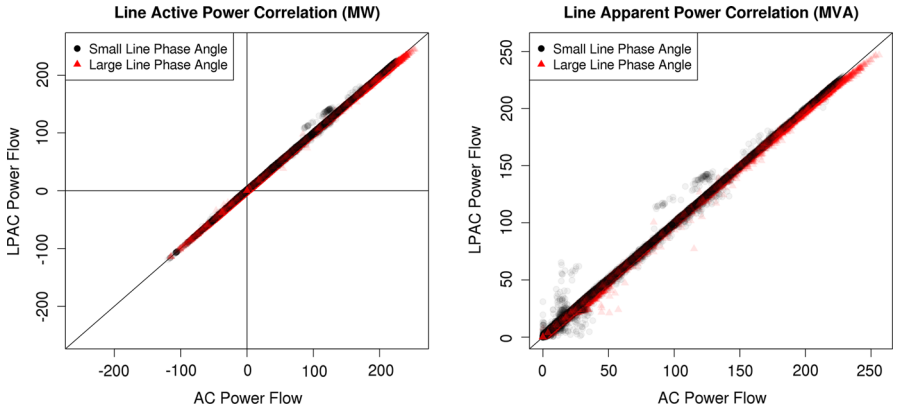

Fig. 4 Accuracy of the DC-LPP model for active and apparent power

significant increase in conversion rate only requires a 10 % reduction in dispatched loads on average.

Consider now the N-10 contingency case to understand the DC-LPP model in more detail. Figure 4 presents correlation plots for active and apparent power for the 8022 converged N-10 contingencies. The results from all contingencies are superimposed onto the same correlation graph and the plots use red triangles for data points obtained

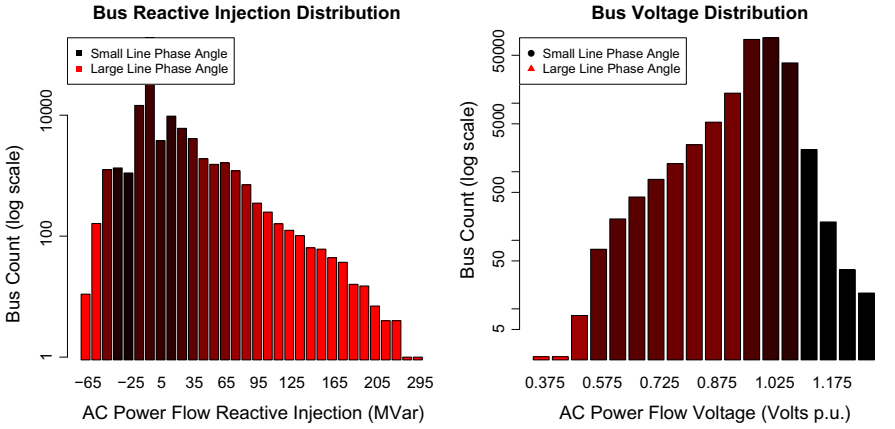

Fig. 5 Reactive injections and voltage magnitudes in the E-DC-LPP algorithm

from networks that feature *large* line phase angles (i.e., $|\theta_n - \theta_m| > \pi/12$). In each plot, the x-axis denotes the values of a measurement (e.g., active power of a line) in the AC solution produced by the E-DC-LPP algorithm while the y-axis the measurement value for the DC-LPP model. As a consequence, the closer a plot is to the line $x = y$, the more the AC and DC solutions agree. Figure 5 presents histograms of the bus reactive injections and voltage magnitudes in the E-DC-LPP solutions. Figures 4 and 5 show that the E-DC-LPP solultions have significant reactive power, extreme reactive injection values (e.g., over 100 MVars), and very low voltage magnitudes (e.g., below 0.8 Volts per unit). Many of the 8022 solved instances are producing extreme and inoperable AC solutions and the remaining unsolved contingencies suffer from unreasonable generator dispatches. The results make clear that, for the LPP, the DC model is inadequate because it does not capture reactive power or voltage magnitudes.

The LPAC model incorporates aspects of reactive power and voltage magnitudes and can impose operational constraints on these values. These additional constraints remove the extreme AC solutions observed in Fig. 5 and produce more reasonable AC solutions at the cost of dispatching slightly less active power. Table 2 has already shown that the E-LPAC-LPP algorithm converges for 99.5 % of the contingencies. Figures 6 and 7 present correlation plots for active, reactive, and apparent power, as well as bus voltages for the E-LPAC-LPP algorithm. The results are encouragingly accurate for the 9971 solved N-10 contingencies. The largest approximation errors occur for bus voltages, which is not surprising since the LPAC model only uses a linear approximation of voltage magnitudes. The reactive injection and voltage magnitudes remain within reasonable bounds (e.g., ± 60 MVar, $\geq$ 0.8 V per unit respectively). Overall, these results indicate that, in this setting, the operational constraints on voltage magnitudes and reactive injections in the LPAC-LPP model effectively constrain the generator dispatches to produce feasible AC power flows.

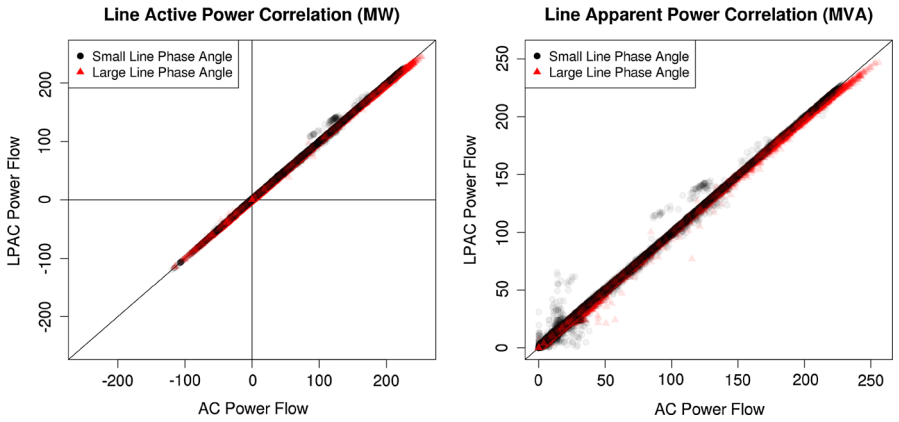

Fig. 6 Accuracy of the LPAC-LPP model for active and apparent power

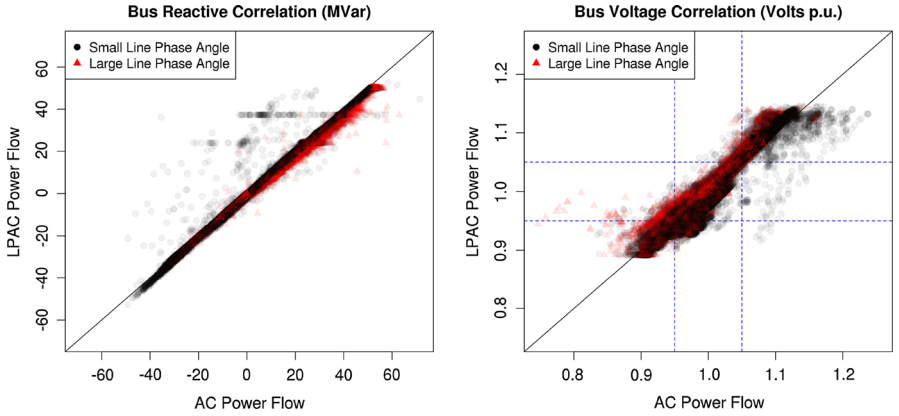

Fig. 7 Accuracy of the LPAC-LPP model for reactive injections and voltage magnitudes

Reliability of the ROP We now study the behavior of the DC-LPP and the LPAC-LPP when used inside the ROP. The analysis is carried out on the 18 PSR benchmarks provided by the Los Alamos National Laboratory (LANL). These benchmarks are based on a US transmission system with 266 components (including loads, generators, lines, and buses) and uses state-of-the-art disaster simulation tools for damage generation [13]. The benchmarks are based on a US transmission system with 266 components (including 54 loads, 33 generators, 106 lines, and 73 buses). The network damages vary significantly across the benchmarks and the most significant damage removes 23 % of the network (61 components).

Once an ordering is chosen, the ROP can be viewed as a sequence of LPPs, which can be used to compare the DC and LPAC models. Since Stage (2) of the E-DC-LPP evaluation fails to converge in numerous cases, the instances are divided into three groups: *Group A* where the E-DC-LPP algorithm always converges to an AC solution; *Group B* where the E-DC-LPP algorithm converges to an AC solution most of the time; *Group C* where the E-DC-LPP algorithm converges so rarely to an AC

Table 3 Quality of the DC-ROP and LPAC-ROP with a fixed restoration order

Model	Inst. solved	Models solved	Violations		
			MLCV	MRIV	MVV
All Instances					
DC	13/18	333/404	301.2	360.6	0.06073
LPAC	18/18	404/404	1.656	13.81	0
Group A—All E-DC-LPP dispatches are AC-feasible					
DC	13/13	196/196	1	330.8	0.0005223
LPAC	13/13	196/196	1.261	12.41	0
Group B—Most DC-LPP dispatches are AC-feasible					
DC	0/3	75/105	203.3	435.1	0.08339
LPAC	3/3	105/105	1.508	14.29	0
Group C—Few DC-LPP dispatches are AC-feasible					
DC	0/2	62/103	331.3	341.4	0.1522
LPAC	2/2	103/103	2.561	15.98	0

In columns 2 and 3, The table reports the number of restoration instances solved without convergence issues and the number of solved LPPs by the DC and LPAC models. The last three columns reports the violations in line capacities, reactive power injections, and voltage bounds

solution that the interpolated restoration plan is worse than the LPAC-LPP plan. Table 3 summarizes the performance of the DC-ROP and LPAC-ROP algorithms. To compare similar LPPs, the ROP is not solved by a MIP solver; rather it is approximated using an ordering heuristic based on operating procedures recommended by the US Department of Homeland Security. The columns in the table are as follows:[3]

1. *Instances solved* The number of benchmarks where the algorithm converge to an AC solution for all the LPPs in the sequence;
2. *Models solved* The total number of LPPs for which the algorithm converges to an AC solution;
3. *Maximum cumulative line capacity violation (MLCV)* The largest cumulative line capacity violation (MVA);
4. *Maximum cumulative reactive injection violation (MRIV)* The largest cumulative generator reactive injection bound violation (MVAr);
5. *Maximum cumulative voltage violation (MVV)* The largest cumulative voltage violation (V p.u.).

The results confirm that the issues plaguing the DC-LPP for the IEEE30 networks carry over to the 18 instances studied here. The E-DC-ROP algorithm produces extreme AC solutions with significant violations of the capacity and voltage constraints. In contrast, the E-LPAC-ROP always converges and produces small violations on capacity and

[3] We use maximum values for the last three measures because the summation and the mean are not particularly meaningful, since the E-DC-ROP algorithm fails to converge to an AC solution on numerous occasions.

Table 4 Comparison of blackout sizes produced by the DC-ROP and LPAC-ROP orderings on a representative subset of the benchmarks

ID	$\|\mathcal{R}\|$	DC-ROP		LPAC-ROP	Relative difference (%)	LPAC-ROP*
		DC-LPP	LPAC-LPP			
1	61	35,320	73,807	47,687	64.61	39,767 (53 %)
16	53	33,104	60,655	53,138	87.61	49,935 (82 %)
3	41	12,906	31,581	22,963	72.71	16,838 (53 %)
13	40	14,655	35,468	31,267	88.15	25,008 (70 %)
12	36	16,954	41,442	41,415	99.94	40,639 (98 %)
2	32	6508	20,515	13, 459	65.60	–
4	24	2245	11,956	5,230	43.75	–

The second column depicts the number of components to repair. The third column gives the size of the blackout for the DC-ROP ordering when evaluated by the DC model. The fourth column gives the size of the blackout for the DC-ROP ordering when evaluated by the LPAC model. The LPAC-ROP gives the size of the blackout for the LPAC-ROP ordering. The fifth column shows the reduction in the blackout size in percentage when using the LPAC ordering instead of the DC-ROP ordering. The last column shows the additional gain (if any) obtained when running the LPAC-ROP algorithm for 8 h

reactive constraint injections. The violations in the E-DC-ROP and E-LPAC-ROP solutions are consistent and of a similar magnitude across all instances.

Impact on the restoration ordering The above results highlight the fact that the load pickups and generator dispatches of the DC-ROP are not reliable. However, this does not imply that the DC-ROP ordering is not of high-quality. We now investigate *whether the DC-ROP is sufficient for selecting a high-quality restoration order.* This would allow the DC-ROP to be used as a first step to find a high-quality ordering before turning to a more accurate model for the final generator dispatches and load pickups.

This section answers this question by comparing the restoration prioritization plans produced by the DC-ROP and LPAC-ROP. Table 4 presents the results on some representative scenarios taken once again from the set of benchmarks provided by LANL. Column 3 depicts the blackout sizes "predicted" by the DC-ROP algorithm: The blackouts are small but Table 3 has already shown that the underlying DC-LPP solutions convert to AC solutions with severe constraint violations. Column 4 depicts the blackout sizes when the orderings produced by the optimal DC-ROP models are evaluated using the LPAC model. Column 5 presents the blackout sizes produced by the LPAC-ROP model. Columns 4 and 5 thus provide a direct way to compare the DC-ROP and LPAC-ROP orderings and the fifth column gives the relative differences between these blackout sizes. The last column gives the results of the LPAC-ROP algorithm when given 8 h of CPU time.

The key message is that the LPAC-ROP orderings are significantly better than those produced by the DC-ROP: The LPAC-ROP always dominates the DC-ROP and the blackout size is reduced by more than half on the last benchmark and by significant percentages in almost all benchmarks. The DC-ROP ordering when evaluated with the LPAC model is in fact producing plans that are similar in quality to the best-practice

heuristic. Columns 3–4 also indicate that DC-LPP significantly underestimates the blackout size. Overall, these results demonstrate the significant benefits of using the LPAC-ROP for the co-optimization of repair prioritizations, load pickups, and generation dispatches. In addition, the results also show that there are considerable benefits in mathematical optimization for minimizing the size of the blackout: Distinct orderings have significant differences in blackout sizes. Finally, the last column shows.

Summary This section considered the ROP, a mixed nonlinear mathematical program for prioritizing repairs. It presented two mixed-integer programming approximations to the ROP: the DC-ROP and the LPAC-ROP. Experimental benchmarks on synthetic benchmarks and real-life power restoration problems demonstrated that the LPAC-ROP produces restoration plans with minimal violations. The DC-ROP in contrast produces plans with very significant violations or plans that cannot be converted in solutions to the AC power flow equations. Moreover, the underlying DC-ROP orderings, when the LPPs are solved with the LPAC-LPP models, are significantly dominated by the LPAC-ROP orderings.

It is useful to discuss the usefulness of the DC model, which is ubiquitous in many power system applications. The DC model is based on assumptions which are typically valid when the power system is operating under "normal" conditions. However, during power restoration, the system is stressed as components are damaged and the goal is to serve as much load as possible to reduce the size of the blackouts. Hence, as the experimental results indicate, the power system exhibits significant reactive power and create severe voltage issues. By modeling reactive power and voltage magnitudes, the LPAC model provides a much more realistic approximation of the power system ouside normal operating conditions.

It is also important to point that ROPs are challenging computationally, as they generalize line-switching problems (e.g., [14,15]). In practice, high-quality solutions are obtained by using a large neighborhood search over the LPAC-ROP MIP model. The large neighborhood search re-optimizes random subsequences, keeping the rest of the schedule fixed. The large neighborhood search uses the linear relaxation at every node of the search. Note however that the linear relaxation is weak for the LPAC-ROP, since it generalizes line-switching [14]. In general, at the root node, the relaxation is zero or close to zero. It is an interesting research topic to derive valid inequalities to strengthen this formulation, an approach pursued for line switching over the DC model in [19].

6 The pickup and repair routing problem

The second stage of the decomposition is the Pickup and Repair Routing Problem (PRRP) which receives, as input, the graph G and the set of precedence constraints $\mathcal{C}$. The PRRP computes a routing plan for the repair crews satisfying the routing constraints specified in Sect. 2 and the precedence constraints $\mathcal{C}$ coming from the ROP. Figure 3 depicts a constraint-programming model for the PRRP, which is almost a direct translation of the problem specifications. To avoid the use of 0/1 variables, it

Model 3 A constraint-programming model for the PRRP.

Inputs:

H^+, H^-	– departure and arrival depots	
W^+	– pickup sites for repairs	
W^-	– repair sites	
V	– vehicles	
$S^+ = H^+ \cup W^+ \cup W^-$		
$S^- = H^- \cup W^+ \cup W^-$		
h_v^+, h_v^-	– departure and arrival depots of vehicle v	
c_v	– capacity of vehicle v	
s_i	– service time at site $i \in W^-$	
d_i	– pickup load at site $i \in W^+$	
$t_{i,j}$	– travel time between sites i and j	
r_i	– repair site associated with pickup site i	
$\mathcal{C}$	– the precedence constraints from the ROP solution	

Variables:

$\sigma_i \in S^-$	– successor of site i	
$vehicle_i \in V$	– vehicle visiting site i	
$weight_i$	– load of the vehicle visiting site i at i	
eat_i	– earliest arrival time at site i	

Minimize:

$$\sum_{i \in W^-} eat_i + s_i \qquad \text{(M3.1)}$$

Subject To:

$alldifferent(\sigma_i \mid i \in S^+)$		(M3.2)
$vehicle_{h_v^+} = v$	$(v \in V)$	(M3.3)
$vehicle_{h_v^-} = v$	$(v \in V)$	(M3.4)
$vehicle_{\sigma_i} = vehicle_i$	$(i \in S^+)$	(M3.5)
$vehicle_{r_i} = vehicle_i$	$(i \in W^+)$	(M3.6)
$weight_i = 0$	$(i \in H^+)$	(M3.7)
$weight_{\sigma_i} = weight_i + d_i$	$(i \in W^+)$	(M3.8)
$weight_{\sigma_i} = weight_i - d_i$	$(i \in W^-)$	(M3.9)
$weight_i \leq c_{vehicle_i}$	$(i \in S^-)$	(M3.10)
$edt_i = 0$	$(i \in H^+)$	(M3.11)
$eat_{\sigma_i} \geq eat_i + t_{i,\sigma_i}$	$(i \in H^+ \cup W^+)$	(M3.12)
$eat_{\sigma_i} \geq eat_i + s_i + t_{i,\sigma_i}$	$(i \in W^-)$	(M3.13)
$eat_{p_i^-} \leq eat_{p_j^-}$	$(i \to j \in \mathcal{C})$	(M3.14)

makes heavy use of the element constraint [35], i.e., the ability to index an array with a decision variable.

Objective (M3.1) minimizes the sum of the repair completion times. Constraints (M3.2) ensures that each site is visited exactly once. Constraints (M3.3–M3.4) ensure that vehicles start at their departure depots and end at their arrival depots. Constraints (M3.5) specify that a site i and its successor are on the same vehicle. Constraints (M3.6) specify that the repair visit is on the same vehicle as its corresponding pickup visit. Constraints (M3.7–M3.10) deal with the vehicle loads and capacities, while constraints (M3.11–M3.14) specify the earliest arrival times and make sure that the pickup visits take place before the repair visit.

Computational considerations As indicated earlier, the PRRP problem is extremely challenging computationally: MIP and constraint-programming solvers have significant difficulties in finding optimal solutions even for small instances. Fortunately, the combination of Constraint Programming (CP) and Large Neighborhood Search (LNS) has been shown particularly effective and scalable in finding high-quality solutions to large-scale complex routing problems (e.g., [5,30]). In the context of the PRRP, LNS selects a set of locations, relaxes the values of their variables and those of their predecessors, and searches for improving solutions in that neighborhood. For this research, we experimented with four neighborhoods.

1. *Random neighborhood (R)* This neighborhood chooses a random set of locations.
2. *Spatial neighborhood (S)* This neighborhood chooses a location l randomly and then selects other locations with a probability inversely proportional to the normalized distance to l.
3. *Temporal neighborhood (T)* This neighborhood chooses a location l randomly and then selects other locations with a probability inversely proportional to the normalized time difference in delivery times with l.
4. *Vehicle neighborhood (V)* This neighborhood selects a number of vehicles (about a quarter of the total vehicles) and selects tasks randomly from these vehicles.

In the rest of the paper, we use LNS(R), LNS(S), LNS(T), and LNS(V) to denote the LNS algorithms over the various neighborhoods. Selecting the sites purely randomly (LNS(R)) was shown to be the most effective strategy [31], dominating spatial, temporal, and vehicle neighborhoods.

However, the LNS algorithm for the PRRP can be improved substantially by using the Randomized Adaptive Decomposition (RAD) scheme proposed in [6]. Given a routing problem $\mathcal{R}$, the key idea in RAD is to use the current solution σ of $\mathcal{R}$ to find a decoupling $(\mathcal{R}_o, \mathcal{R}_s)$ with projected solution σ_o and σ_s. Subproblem $\mathcal{R}_o$ is then reoptimized and its solution is merged with σ_s to obtain a new solution to $\mathcal{P}$. More precisely, the RAD is based on two principles:

1. Starting from plan σ_0, it produces a sequence of plans $\sigma_1, \ldots, \sigma_j$ such that $f(\sigma_0) \geq f(\sigma_1) \geq \cdots \geq f(\sigma_j)$.
2. At step i, the scheme uses σ_{i-1} to obtain a decoupling $(\mathcal{R}_o, \mathcal{R}_s)$ of $\mathcal{R}$ with projected solutions σ_o and σ_s. It reoptimizes $\mathcal{R}_o$ to obtain σ_o^* and the new plan $\sigma_i = \text{MERGE}(\sigma_o^*, \sigma_{i-1})$

The main difference between LNS and RAD is the fact that the problem is fully decomposed and hence it has a smaller search space: Other parts of the routing are not considered as reinsertion points for the visits. One of the most challenging aspects of RAD is how to merge decoupled solutions, i.e, $\sigma_i = \text{MERGE}(\sigma_o^*, \sigma_{i-1})$. In [6], this challenge is addressed by choosing $\mathcal{R}_o$ such that the customers of entire vehicles are removed. The merging operation is then trivial, since the vehicles in $\mathcal{R}_o$ and $\mathcal{R}_s$ are disjoint. More sophisticated, temporal and spatial, decouplings were also explored in [7]. Precedence constraints in the PRRP complicate the more sophisticated decompositions and may also make spatial decompositions much less effective. As a result, our PRRP algorithm considers a randomized adaptive vehicle decomposition (RAVD): Each step chooses a quarter of the vehicles randomly and then runs LNS(R) on the

Table 5 Quality of the greedy, LNS, and RAVD Solutions for the PRRP

Instance name	$\|R\|$	H.	Greedy	LNS(R)	RAVD	%Greedy	%LNS(R)
BM2-h15	67	1	134,837	110,860	107,320	20.41	3.19
BM2-h09	86	1	184,894	150,780	148,300	19.79	1.64
BM2-h03	100	1	286,071	227,390	220,395	22.96	3.08
Average						21.05	2.64
BM3-h15	53	1	67,012	57,768	48,248	28.00	16.48
BM3-h00	61	1	92,512	81,234	70,079	24.25	13.73
Average						26.12	15.11
BM4-h16	54	2	84,230	65,741	54,730	35.02	16.75
BM4-h15	97	2	261,220	220,140	163,820	37.29	25.58
BM4-h09	106	2	307,171	246,990	182,490	40.59	26.11
BM4-h03	121	2	437,972	354,570	264,690	39.56	25.35
Average						38.12	23.45
BM5-h03	206	8	1,307,329	1,033,600	674,320	48.42	34.76
BM5-h11	255	8	2,248,539	1,779,900	1,133,900	49.57	36.29
BM5-h17	432	8	6,341,765	5,998,400	5,150,500	18.78	14.14
BM5-h00	439	8	6,782,781	6,189,600	4,609,600	32.04	25.53
BM5-h05	504	8	9,112,107	8,220,600	6,072,100	33.36	26.14
Average						36.43	27.37
BM5-h05	504	20	9,112,107	7,958,400	5,433,300	40.37	31.73

The second column gives the number of damaged components. The third column the time limit in hours. The next three columns report the best-found objective value for the greedy, LNS, and RAVD algorithms. The last two columns give the improvements in percentage of the RAVD algorithm compared to the greedy and LNS approaches

subproblem consisting of those vehicles and their jobs. In the subproblem, precedence constraints are imposed between the jobs. Moreover, like in [26], the decomposition imposes some temporal constraints on the jobs to ensure that optimizing the subproblem does not degrade the overall objective function. In particular, the jobs have a constraint on their earliest and latest arrival times computed from the precedence constraints linking the selected and remaining vehicles.

Benchmarks The PRRP model was also evaluated on benchmarks produced by the Los Alamos National Laboratory and based on the electrical infrastructure of the United States. The disaster scenarios were generated using state-of-the-art hurricane simulation tools used by the National Hurricane Center [13,27]. The damages in the scenarios vary considerably, from about 50 to 500 components to repair, inducing between about 100 and 1000 routing visits. There are between 10 and 15 trucks on these instances. The scenarios represent power restoration problems at the scale of a US state (e.g., Florida) and are thus of significant computational complexity. Instances with less than 100 damaged components focus on the transmission network alone, while those with 500 damaged items incorporate aspects of both the transmission and distribution

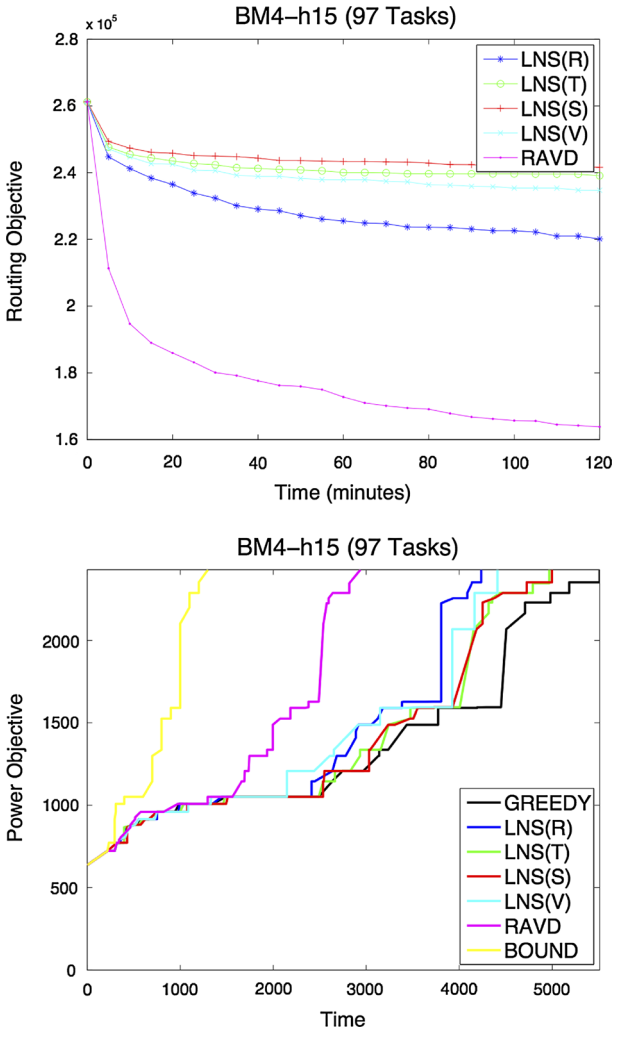

Fig. 8 The routing objective and the blackout size over time: 97 jobs

networks. For this paper, we used a total of 15 representative disaster contingencies. For each instance, the current "best practice" in the field serves as a baseline. The "best practice" implements a restoration order dictated by the US government and based on network utilization heuristics. It then uses an agent-based greedy routing algorithm that satisfies the restoration order. The algorithms all use the best-practice solution (which is fast to compute) as a starting point, which is depicted as the left-most point in the graphs. The experiments were run on quad-core Dell PowerEdge 1855 blade systems with Xeon 2.8 processors. The execution times vary from 1 to 20 h depending on the instance size. The results are the average over 10 executions for each benchmark and configuration. Recall that, when the objective is to minimize the average delivery

time, Campbell et al. [9] have shown that MIP approaches have serious scalability issues, even on small instances.

Quality of the results Table 5 presents a summary of the quality results. For each benchmark, the table gives the number of damaged components (column $|R|$), the number of hours the optimization algorithm was run (column $H.$), the "Best Practice" solution (column Greedy), the LNS from [36] [column LNS(R)], and the randomized adaptive decomposition (RAVD). The table also gives the percentage improvement of RAVD with respect to the "best practice" (%Greedy) and the LNS(R) [%LNS(R)] solutions. There is a line for each benchmark and an average for each benchmark class (e.g., BM2) which corresponds to a specific network. The last line reports the results of benchmark BM5-h05 when run for 20 h. The results indicate that RAVD brings substantial benefits over LNS(R) and that these benefits increase with the size of the damages. On the BM5 benchmark class, the improvement is about 27% in average, which is substantial. Overall, RAVD brings significant benefits in solution quality over large neighborhood search and tremendous improvements over "best practices".

It is interesting to look at specific benchmarks to visualize these results in more detail. Figure 8 depicts the results on the BM4-h15 benchmark which is relatively small. The left graph compares the solution quality of various LNS algorithms and the RAVD algorithm over time. It highlights the significant benefits of RAVD in solution quality and its speed in finding high-quality solutions. The right graph depicts the size of the blackouts resulting from the various algorithms. It also shows a very crude lower bound obtained by ignoring travel distances, i.e., viewing the problem as a pure restoration without taking account the travel times of repair crews. The results show that RAVD almost cuts in half the gap between the crude lower bound and the LNS(R) algorithm, giving some indirect evidence of its quality beyond its improvement over the "best practice" in the field.

7 Conclusion and future work

This paper showed how mathematical programming provides significant benefits for the repair and restoration of a transmission system after a significant disruption. It considered the TSRRP which consists in dispatching crews to repair damaged electrical components in order to minimize the size of the blackout. The TSRRP can be modeled as a large-scale mixed nonlinear, nonconvex program, including both routing components and the nonlinear steady-state power flow equations. To tackle its daunting computational complexity, this paper proposed a 2-stage approach, decoupling the restoration and repair aspects. The first step is a restoration ordering problem, a mixed nonlinear, nonconvex program which is approximated by a mixed integer program. The approximation does not use the traditional DC power flow approximation which is plagued by convergence issues and inoperable dispatches; rather, it uses the recent LPAC approximation that captures reactive power and voltage magnitudes. The second stage is a pickup and repair routing problem which is solved using a constraint-programming model, large neighborhood search, and a randomized adaptive decomposition. Experimental results on benchmarks based on the US elec-

trical infrastructures and state-of-the-art damage scenarios indicate that the 2-stage approach provides significant improvements over the "best practice" in the field.

The experimental results have also shown that the traditional DC model is not appropriate for the TSRRP, as it often overestimates the load that can be pushed in the power network. Its load pickups and generation dispatches often cannot be converted to AC solutions or they produce inoperable dispatches that severely violates thermal and voltage constraints. In contrast, the LPAC model, because of its ability to capture reactive power and voltage magnitudes, can be used to produce AC solutions with no or minimal constraint violations.

There are many directions for further work. At the modeling level, it is necessary to generalize the model to include more operational aspects such as generator ramp rates (e.g., [33]). It is also important to ensure that the restoration actions do not endanger the stability of the networks. Recent work [16,21] has shown some progress in this direction, although applicability to large-scale networks is an open issue. Finally, the joint restoration of transmission and distribution networks is a key research avenue: The present work models distribution networks as loads in the transmission systems but this is a coarse approximation and it needs to be reconsidered.

On the computational side, the use of quadratic approximation and global optimization could bring some additional benefits. A quadratic approximation would capture voltage magnitudes more precisely, while global optimization will be helpful in providing both lower and upper bounds on the size of the blackouts. Both of these topics are being investigated.

Acknowledgments We would like to thank the reviewers for many interesting comments and suggestions that improve the paper significantly. NICTA is funded by the Australian Government through the Department of Commu- nications and the Australian Research Council through the ICT Centre of Excellence Program.

References

1. Adibi, M.: Power System Restoration: Methodologies & Implementation Strategies. IEEE Press, New York (2000)
2. Adibi, M.M., Fink, L.H.: Power system restoration planning. IEEE Trans. Power Syst. **9**(1), 22–28 (1994)
3. Adibi, M.M., Kafka, L.R.J., Milanicz, D.P.: Expert system requirements for power system restoration. IEEE Trans. Power Syst. **9**(3), 1592–1600 (1994)
4. Ancona, J.J.: A framework for power system restoration following a major power failure. IEEE Trans. Power Syst. **10**(3), 1480–1485 (1995)
5. Bent, R., Van Hentenryck, P.: A two-stage hybrid local search for the vehicle routing problem with time windows. Transp. Sci. **8**(4), 515–530 (2004)
6. Bent, R., Van Hentenryck, P.: Randomized adaptive spatial decoupling for large-scale vehicle routing with time windows. In: Proceedings of the Twenty-Second Conference on Artificial Intelligence, Vancouver, Canada (AAAI'07) (2007)
7. Bent, R., Van Hentenryck, P.: Spatial, temporal, and hybrid decompositions for large-scale vehicle routing with time windows. In: Cohen, D. (ed.) CP, Volume 6308 of Lecture Notes in Computer Science, pp. 99–113. Springer, Berlin (2010)
8. Bienstock, D., Mattia, S.: Using mixed-integer programming to solve power grid blackout problems. Discrete Optim. **4**(1), 115–141 (2007)
9. Campbell, A.M., Vandenbussche, D., Hermann, W.: Routing for relief efforts. Transport. Sci. **42**(2), 127–145 (2008)

10. Coffrin, C., Van Hentenryck, P., Bent R.: Strategic stockpiling of power system supplies for disaster recovery. In: Proceedings of the 2011 IEEE Power & Energy Society General Meetings (PES) (2011)
11. Coffrin, C., Van Hentenryck, P.: A linear-programming approximation of AC power flows. INFORMS J. Comput. **26**(4), 718–734 (2014)
12. Delgadillo, A., Arroyo, J.M., Alguacil, N.: Analysis of electric grid interdiction with line switching. IEEE Trans. Power Syst. **25**(2), 633–641 (2010)
13. FEMA: FEMA HAZUS Overview. www.fema.gov/plan/prevent/hazus (2010)
14. Fisher, E.B., O'Neill, R.P., Ferris, M.C.: Optimal transmission switching. IEEE Trans. Power Syst. **23**(3), 1346–1355 (2008)
15. Hijazi, H.L., Coffrin, C., Van Hentenryck, P.: Convex quadratic relaxations of mixed-integer nonlinear programs in power systems. Technical Report—NICTA, Canberra ACT, Australia (2013)
16. Hijazi, H., Mak, T., Van Hentenryck, P.: Power system restoration with transient stability. In: Proceedings of the Twenty-Ninth AAAI Conference on Artificial Intelligence (AAAI-15), Austin, Texas (2015)
17. Huang, J.A., Galiana, F.D., Vuong, G.T.: Power system restoration incorporating interactive graphics and optimization. In: Proceedings of the IEEE Power Industry Computer Application Conference, pp. 216–222. Baltimore, MD (1991)
18. Huang, J.A., Audette, L., Harrison, S.: A systematic method for power system restoration planning. IEEE Trans. Power Syst. **10**(2), 869–875 (1995)
19. Jeon, H., Linderoth, J., Luedtke, J.: Valid inequalities for potential-constrained network design. Presented at MINLP, CMU, Pittsburgh, PA (2014)
20. Knight, U.: Power Systems Engineering and Mathematics. Pergamon Press, Oxford (1972)
21. Mak, T., Coffrin, C., Van Hentenryck, P., Hiskens, I., Hill, D.: Power system restoration planning with standing phase angle and voltage difference constraints. In: Proceedings of the 18th Power Systems Computation Conference (PSCC-14), Wroclaw, Poland (2014)
22. Morelato, A.L., Monticelli, A.J.: Heuristic search approach to distribution system restoration. IEEE Trans. Power Deliv. **4**(4), 2235–2241 (1989)
23. Mori, H., Ogita, Y.: A parallel tabu search based approach to optimal network reconfigurations for service restoration in distribution systems. In: Proceedings of the 2002 IEEE International Conference on Control Applications, vol. 2, pp. 814–819 (2002)
24. Nagata, T., Sasaki, H., Yokoyama, R.: Power system restoration by joint usage of expert system and mathematical programming approach. IEEE Trans. Power Syst. **10**(3), 1473–1479 (1995)
25. Overbye, T.J., Cheng, Xu, Sun, Yan: A comparison of the ac and dc power flow models for lmp calculations. In: Proceedings of the 37th Annual Hawaii International Conference on System Sciences (2004)
26. Pacino, D., Van Hentenryck, P.: Large neighborhood search and adaptive randomized decompositions for flexible jobshop scheduling. In: Walsh, T. (ed.) IJCAI, pp. 1997–2002. IJCAI/AAAI, Barcelona, Spain (2011)
27. Reed, D.A.: Electric utility distribution analysis for extreme winds. J. Wind Eng. Ind. Aerodyn. **96**(1), 123–140 (2008)
28. Sakaguchi, T., Matsumoto, K.: Development of a knowledge based system for power system restoration. IEEE Trans. Power Appar. Syst. **PAS–102**(2), 320–329 (1983)
29. Salmeron, J., Wood, K., Baldick, R.: Worst-case interdiction analysis of large-scale electric power grids. IEEE Trans. Power Syst. **24**(1), 96–104 (2009)
30. Shaw, P: Using constraint programming and local search methods to solve vehicle routing problems. In: Proceedings of Fourth International Conference on the Principles and Practice of Constraint Programming (CP'98), pp. 417–431. Springer (1998)
31. Simon, B., Coffrin, C., Van Hentenryck, P.: Randomized adaptive vehicle decomposition for large-scale power restoration. In: Beldiceanu, N., Jussien, N., Pinson, E. (eds.) CPAIOR, Volume 7298 of Lecture Notes in Computer Science, pp. 379–394. Springer, Berlin (2012)
32. Stott, B., Jardim, J., Alsac, O.: Dc power flow revisited. IEEE Trans. Power Syst. **24**(3), 1290–1300 (2009)
33. Sun, W., Liu, C.C., Zhang, L.: Optimal gnerator start-up strategy for bulk power system restoration. IEEE Trans. Power Syst. **26**(3), 1357–1366 (2011)
34. Tamura, Y., Mori, H., Iwamoto, S.: Relationship between voltage instability and multiple load flow solutions in electric power systems. IEEE Trans. Power Appar. Syst. **PAS–102**(5), 1115–1125 (1983)
35. Van Hentenryck, P.: Constraint Satisfaction in Logic Programming. The MIT Press, Cambridge (1989)

36. Van Hentenryck, P., Coffrin, C., Bent, R.: Vehicle routing for the last mile of power system restoration. In: Proceedings of the 18th Power Systems Computation Conference (PSCC'11), Stockholm, Sweden (2011)
37. Wächter, A., Biegler, L.T.: On the implementation of a primal-dual interior point filter line search algorithm for large-scale nonlinear programming. Math. Program. **106**(1), 25–57 (2006)
38. Yolcu, M.H., Zabar, Z., Birenbaum, L., Granek, S.A.: Adaptation of the simplex algorithm to modeling of cold load pickup of a large secondary network distribution system. IEEE Trans. Power Appar. Syst. **102**(7), 2064–2068 (1983)